Journal of Nuclear Materials 425 (2012) 140–146

Contents lists available at SciVerse ScienceDirect

Journal of Nuclear Materials

journal homepage: www.elsevier.com/locate/jnucmat

Radiation damage in helium ion irradiated nanocrystalline Fe

K.Y. Yu [a], Y. Liu [a], C. Sun [a], H. Wang [b], L. Shao [c], E.G. Fu [d], X. Zhang [a,*]

[a] Department of Mechanical Engineering, Materials Science and Engineering Program, Texas A&M University, College Station, TX 77843-3123, United States
[b] Department of Electrical and Computer Engineering, Texas A&M University, College Station, TX 77843-3128, United States
[c] Department of Nuclear Engineering, Texas A&M University, College Station, TX 77843-3133, United States
[d] Materials Physics and Applications Division, Los Alamos National Laboratory, Los Alamos, NM 87545, United States

ARTICLE INFO

Article history:
Available online 16 November 2011

ABSTRACT

Fe films with an average columnar grain size varying from 49 to 96 nm are deposited by magnetron sputtering technique. Sputtered films have predominant body centered cubic structure together with a small fraction of face centered cubic phase. Bulk Fe with an average grain size of 700 nm is also irradiated at the same condition for comparison. Helium bubbles are observed in Fe films and bulk Fe irradiated by 100 keV helium ions to a fluence of 6×10^{20} ions/m^2 at room temperature. Smaller grains lead to lower density of He bubbles. Radiation hardening in Fe films is much less than that of bulk Fe, and is a combined consequence of He bubble induced hardening and radiation induced compressive stress in Fe films.

1. Introduction

Energetic particles during radiation interact with atoms of the target material and induce a large number of point defects, such as vacancies and interstitials. Point defects aggregate to form vacancy clusters, voids, dislocation loops and stacking fault tetrahedron [1–4]. Void swelling and He embrittlement may lead to severe degradation of mechanical properties [5,6]. It is of great interest to develop radiation tolerant materials that can promote the annihilation of radiation induced defects. Studies have shown that certain grain and phase boundaries may act as preferential trapping sites for irradiation induced point defects and their clusters, promote recombination of interstitials and vacancies, and thus alleviate the degradation of mechanical properties [7,8]. It has been established that He plays an important role on the evolution of microstructures and mechanical properties of irradiated materials [9–11]. Helium, in existence of high concentration of vacancy clusters, can quickly combine with vacancy clusters to form He bubbles [6]. Bubble density in some of He ion irradiated metals can approach 10^{23}/m^3 or greater [12,31,33]. Understanding these phenomena is important to develop radiation tolerant materials.

Since stainless steels are commonly used as nuclear reactor structural components, its matrix element, Fe, has been investigated extensively for radiation response [13–17]. He implantation induced radiation damage in Fe has been widely studied by modeling and simulation, including the formation and diffusion of He clusters and bubbles [18,20], He-grain boundary interactions [21,22,36], He-dislocation interactions [23], He cluster thermal stability [24,27] and bubble pressure and size [28]. These studies have demonstrated that He atoms can be absorbed by both dislocations and grain boundaries. He has a higher binding energy to grain boundaries due to their greater excess volume [11,36]. Bubble density and size are related to grain boundary structures [19,21]. Experimentally, He desorption has been investigated in both single crystal and polycrystalline Fe [26,29], where polycrystals are found to be more favorable for He absorption.

Nanostructured materials have high volume fraction of interfaces, including high angle grain boundaries, phase boundaries and layer interfaces. These high energy defects may act as point defect sinks and thus lead to enhancement of radiation tolerance [3,25,30]. Recent studies show that Cu/Nb, Cu/V and Fe/W multilayer films can significantly reduce radiation induced defects due to their abundant interfacial area [30–34]. Size dependent reductions of He bubble density, lattice distortion, swelling as well as radiation hardening have been observed in He ion irradiated Cu/V multilayers [31,32]. Furthermore the study of He ion irradiated Cu/Mo multilayers shows that segregation of He bubbles to interfaces is directly related to the vacancy-to-He concentration ratio [33]. A relatively low concentration of vacancies allows He to diffuse to the interface and form He bubbles at interfaces. Another type of boundary, metal/oxide interface, can also dramatically enhance radiation tolerance. Uniformly distributed nanoscale oxide precipitates in oxide-dispersion-strengthened (ODS) alloys, have shown superior void swelling resistance and high temperature thermal stability [14]. Nanocrystalline Fe and its alloys subjected to different heavy ion (Kr) radiations have been investigated by Karpe et al., who showed that Kr ions could trigger faster grain growth because of denser collision cascade [35]. Size dependent radiation response has also been found in He irradiated stainless steel, in terms of delayed void nucleation, lower void densities and reduced void swelling by decreasing grain size [8]. It has also

* Corresponding author. Tel.: +1 979 845 2143.
E-mail address: zhangx@tamu.edu (X. Zhang).

0022-3115/$ - see front matter © 2011 Elsevier B.V. All rights reserved.
doi:10.1016/j.jnucmat.2011.10.052

been shown that the binding energy of He with grain boundaries increases linearly with grain boundary excess volume, which means high volume fraction of grain boundary may trap more He atoms [36]. Despite the aforementioned studies, He ion induced damage in nanocrystalline Fe films has rarely been studied experimentally. In this paper, we present the study of radiation induced defects (mainly He bubbles) and the evolution of mechanical properties in nanocrystalline Fe film. Bulk Fe with large grain size is also irradiated for comparison. This study helps to understand the role of grain boundaries on reducing He induced radiation damage in metals.

2. Experimental

Nanocrystalline Fe films with thickness of ~1 μm were synthesized on oxidized silicon (SiO_2) substrates by using DC magnetron sputtering technique at room temperature. The deposition rate was varied from 0.36 to 0.71 nm/s in order to tailor the average grain size. The purity of the Fe target is 99.95%. A base pressure of 6.7×10^{-6} Pa was reached before depositions and the Ar partial pressure during sputtering was ~0.5 Pa. Before and after deposition, the curvature of substrate was measured by using a Dektak 150 Stylus profilometer with a Z height resolution of ~0.5 nm. Prior to He ion irradiation, the samples were partially masked so that swelling can be measured by the profilometer. The Fe films with various grain sizes were irradiated together at room temperature using 100 keV He ions. A total fluence of 6×10^{20} ions/m^2 was achieved in 2 h at a constant beam current of 5.1 μA. The temperature rise of the sample stage was ~50 °C during implantation. Base pressure in the ion implanter was 4×10^{-5} Pa. A piece of bulk Fe was cut from the sputtering target mentioned above. The bulk Fe was then irradiated separately, using the same condition as Fe films.

The microstructure of Fe films was characterized by a Bruker-AXS D8 advanced Bragg–Brentano X-ray powder diffractometer with $\lambda_{K\alpha 1}$ = 0.154056 nm. The cross-sectional transmission electron microscopy (XTEM) samples were mechanically ground and polished, followed by dimpling and low energy (3.5 keV) Ar ion milling. XTEM samples were then examined by a 200 kV JEOL 2010 transmission electron microscope equipped with a Gatan SC1000 ORIUS CCD camera. During TEM sample preparation Ar ion milling can induce damage in the form of Ar bubbles and amorphization. These artifacts were typically observed in a narrow region, within 20 nm from the edge of TEM specimens (near the center of a hole in specimens). Appropriate selection of ion milling parameters (low energy and low angle), can effectively reduce the ion milling induced damage [32]. The indentation hardness and modulus of the Fe films were measured based on an average of 12–15 indents at different indentation depths at room temperature, by a Fischerscope HM2000XYp micro/nanoindenter with a Vickers indenter tip. The loading rate was kept at 10 mN/s and maximum indentation depth was ~150 nm for all film specimens and ~250 nm for bulk specimen.

3. Results

X-ray diffraction (XRD) spectra of the as-deposited Fe films at different deposition rate are shown in Fig. 1 by thicker solid lines. Strong bcc (1 1 0) texture is observed in Fe films, and bcc (1 1 0) peaks in all specimens deviate slightly from the standard position, as indicated by the vertical dash line. Such deviation implies the existence of residual stress in the as-deposited film, which will be discussed later. Furthermore these as-deposited films also show a small shoulder peak, identified to be fcc (1 1 1) Fe. After He ion irradiation, the XRD spectra (thinner lines) show insignificant

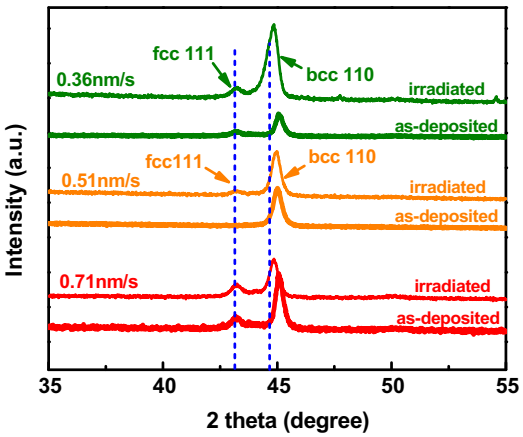

Fig. 1. XRD patterns of as-deposited and He ion irradiated Fe films synthesized at the deposition rate of 0.36, 0.51 and 0.71 nm/s. Films have strong bcc (1 1 0) texture together with a small fcc (1 1 1) shoulder peak. The bcc peak of as-deposited film is to the right of the standard position (vertical dash line), and after radiation the peak positions shift to lower angles.

changes of relative peak intensity, but the bcc (1 1 0) peaks of all irradiated films became closer to the standard position ($d^{bulk}_{(1\,1\,0)}$ = 0.2025 nm).

XTEM micrographs of the as-deposited films (Fig. 2a and b) shows numerous columnar grains along the growth direction. Selected area diffraction (SAD) patterns (insets in Fig. 2a and b), collected by a large aperture to include numerous grains, reveal the coexistence of the bcc (1 1 0) and fcc (1 1 1) orientations consistent with XRD analysis. Plan-view TEM micrograph of bulk Fe with large grains is shown in Fig. 2c. Grain size distributions are shown in Fig. 2d–f. For films, a doubling of deposition rate from 0.36 to 0.71 nm leads to a twofold reduction of average columnar grain size, from 96 to 49 nm. The average grain size of films deposited at a rate of 0.51 nm/s is ~66 nm. In the remainder of this paper, we will use average grain size to differentiate the three Fe films, wherein 96 nm Fe refers to Fe films with an average grain size of 96 nm. Average grain size of bulk Fe is ~700 nm, as shown in Fig. 2e. Profilometer studies did not detect noticeable swelling in any irradiated Fe films.

The stopping and range of ions in matter (SRIM) computer code [37] was used to simulate the profiles of He concentration and displacements in Fe as a function of depth. The threshold displacement energy for Fe is 40 eV [6]. The simulation, as shown in Fig. 3, implies the He concentration reaches a peak value of ~4 at.% at a depth of ~340 nm. The peak irradiation damage is approximately six displacements per atom (dpa) at a depth of ~290 nm and the irradiated region extends to a maximum depth of ~480 nm underneath the surface.

Under-focused XTEM micrograph of irradiated 49 nm Fe films is shown in Fig. 4a. The micrograph was collected in the peak damages regions, which are ~300 nm deep. We observed high density of He bubbles within the columnar grains. Meanwhile, arrays of bubbles formed along grain boundaries, as indicated by arrows in the magnified XTEM micrograph in Fig. 4b. XTEM micrographs were taken at an under-focus distance of ~400 nm to estimate the average He bubble size. As shown in Fig. 4c and d, The 49 nm Fe film has a slightly smaller average bubble diameter, ~1.1 nm, in comparison to ~1.3 nm bubble size in 96 nm Fe film. However, the average bubble diameter of bulk Fe is 1.1 nm in comparison.

The density of He bubbles at different depth was measured via extensive XTEM studies. The thickness of TEM foil was measured by using the Kossel–Mollenstedt fringes under two beam conditions. Calculation shows that the TEM foil thickness is ~138, 87